

Are your MRI contrast agents cost-effective?

Learn more about generic **Gadolinium-Based Contrast Agents**.



**FRESENIUS
KABI**

caring for life

AJNR

Pseudoatrophy of the cervical portion of the spinal cord on MR images: a manifestation of the truncation artifact?

D M Yousem, P A Janick, S W Atlas, D B Hackney, S A Glasser, F W Wehrli and R I Grossman

This information is current as of March 21, 2025.

AJNR Am J Neuroradiol 1990, 11 (2) 373-377
<http://www.ajnr.org/content/11/2/373>

Pseudoatrophy of the Cervical Portion of the Spinal Cord on MR Images: A Manifestation of the Truncation Artifact?

David M. Yousem¹
 Peter A. Janick¹
 Scott W. Atlas¹
 David B. Hackney¹
 Scott A. Glasser²
 Felix W. Wehrli¹
 Robert I. Grossman¹

Routine evaluation of axial MR images of the cervical spine with high-intensity CSF (long TR/TE spin-echo or gradient-echo images) revealed apparent narrowing of the cord's anteroposterior diameter when these images were compared with corresponding postmyelography CT scans. This discrepancy was believed to be due to the truncation artifact at the CSF-cord boundary. To examine the truncation effect, we compared cord diameters in 12 patients on postmyelography CT scans and MR images and then compared these with MR scans of normal volunteers and of an agar-saline spine phantom. There was an artifactual diminution of the cord diameter in the 128-step phase-encoding axis of the 128 × 256-matrix MR scan as compared with the diameter of the cord in the patients' postiohexol CT scans and in the 256 phase-encoded axis MR scan in the volunteer study. A similar discrepancy was noted in the spine phantom study, in which the cord diameter in the 256-step phase-encoded MR scan, the CT scan, and direct measurement exceeded that in the 128-step phase-encoded axis MR scan. The range of differences between the measurements was as large as 2.3 mm (patients), 1.7 mm (volunteers), and 1.8 mm (phantom) for the three studies. In all three studies, varying the photographic window width and level produced variation in the apparent cord diameter of up to 1.5 mm. To eliminate this effect, the cord diameters in the phantom and the normal control subjects were measured at identical window levels.

The truncation artifact, coupled with standard window settings used in photography, may lead to inaccurate display of the diameter of the cervical spinal cord.

AJNR 11:373-377, March/April 1990; *AJR* 154: May 1990

During routine evaluation of MR images of the cervical spine obtained with either conventional spin-echo or 3D Fourier transformation (3DFT) gradient-echo sequences in which CSF was hyperintense, a discrepancy was noted in the apparent size of the anteroposterior (AP) diameter of the cervical spinal cord compared with postmyelography axial CT scans obtained in the same patient (Fig. 1). The spinal cord appeared smaller on the MR images. It was hypothesized that the truncation artifact at the interface of hyperintense CSF and hypointense spinal cord was responsible for the misrepresentation of the cord size. By comparing the MR images with postintrathecal contrast CT scans and examining the effects of matrix size and phase-encoding direction in normal volunteers and in a spine phantom, we developed an explanation for the mechanism for the incongruity of the measured cervical spinal cord dimensions.

Subjects and Methods

Clinical Patients

The axial scans of 12 consecutive patients who had an MR scan with hyperintense CSF (i.e., either a long TR/TE spin-echo or a low flip angle gradient-echo MR scan) and a postmyelography CT scan with the same scan angulation within a period of 6 weeks were retrospectively reviewed by three neuroradiologists. The MR scans were obtained on a 1.5-

Received May 22, 1989; revision requested July 27, 1989; revision received October 2, 1989; accepted October 10, 1989.

Presented at the annual meeting of the American Society of Neuroradiology, Orlando, March 1989.

¹ Department of Radiology, Neuroradiology Section, Hospital of the University of Pennsylvania, 3400 Spruce St., Philadelphia, PA 19104. Address reprint requests to S. W. Atlas.

² Department of Radiology, Albert Einstein Medical Center, Philadelphia, PA 19141.

0195-6108/90/1102-0373

© American Society of Neuroradiology

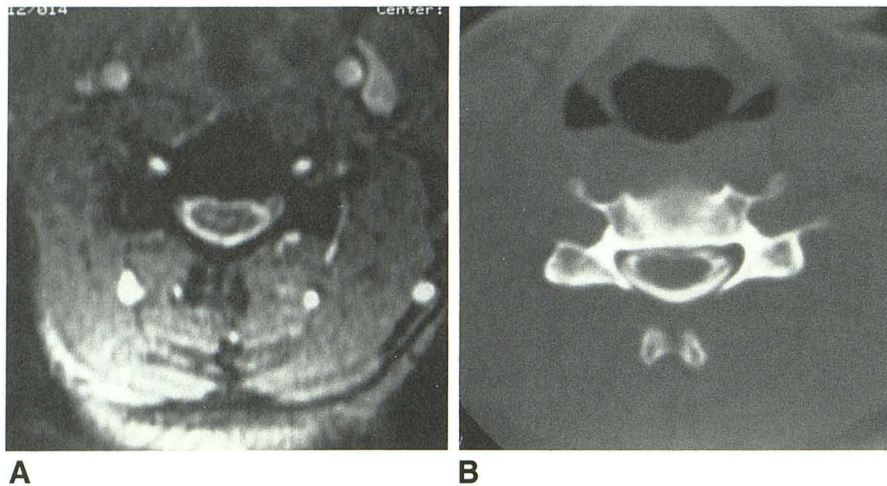


Fig. 1.—MR vs postmyelography CT of C5 AP diameter.

A, Axial gradient-echo 3DFT MR image.

B, Axial CT scan after intrathecal contrast administration.

The gradient-echo image (A) demonstrates a 1.3-mm difference in AP cord diameter as compared with postmyelography CT scan (B) taken 2 weeks later at the same plane and angulation. Cord atrophy might have been suspected on the MR study if one had not been cognizant of the truncation artifact in the 128 AP axis.

T GE imaging system employing a 5-in. round surface coil. Long TR/TE spin-echo scans had TRs greater than 2000, TEs of 50 or greater, 3–5-mm slice thicknesses, and 16–24-cm fields of view (FOV). The MR gradient-echo 3DFT gradient-recalled acquisition in the steady state (GRASS) volumetric sequences were obtained with flip angles of 5° with 50/15/1 (TR/TE/excitations), 1.5-mm contiguous slices, a 128 × 256 matrix (the 128-phase axis in the AP direction), 64 slice encodings, and a 24-cm field of view. Velocity compensation (first-order gradient moment nulling) was employed on all sequences. The CT scans were obtained on a GE 9800 scanner after the intrathecal administration of iohexol (240–300 mg/dl). Slice thickness was 3 mm, and scans were photographed at soft-tissue and bone-window settings.

Measurements of the cervical spinal cord were obtained in the AP dimension for equivalent levels on the CT and MR images. Thirty levels in 12 patients were independently evaluated by three radiologists. Direct measurements from hard copy images were made with calipers and were rounded to the nearest 0.5 mm.

Normal Volunteers

To corroborate the conjecture that the truncation artifact was responsible for the discrepancy in cord dimensions on MR images, we compared MR scans on three normal volunteers obtained with a gradient-echo 3DFT volumetric sequence with a 128 × 256 and a 256 × 256 matrix. Pixel sizes were 1.875 mm and 0.9375 mm when 128 and 256 encoding steps were used, respectively, with this 24-cm FOV sequence. Additionally, 3DFT scans were obtained in which the orientation of the 128 axis of the 128 × 256 matrix was designated AP and then right-left. AP cord diameters were measured at random slice sections. The results of the cord dimensions on the three separate sequences, as measured by a single radiologist using electronic calipers on the viewing screen, were then compared.

Phantom Study

A phantom consisting of a 7.3-mm inner core of agar in dialysis tubing surrounded by an outer concentric tube of normal saline and floating in tap water was used to simulate the intensity characteristics of the CSF and spinal cord. This phantom was scanned with identical MR parameters used for the normal volunteer study. The number of phase-encoding steps, and the orientation of the 128-step phase and frequency axes, were varied in a similar fashion to the volunteer study described above. AP diameters were again measured by one

radiologist at 16 random levels. The phantom was also scanned by CT to ascertain CT dimensions of the concentric tubes. Direct measurement of the diameter was also performed at the corresponding levels.

Results

Table 1 provides a summary of the results described in this section.

Clinical Patients

In 52 of 90 patient levels (30 levels measured by three radiologists), the AP diameter of the cervical cord as measured on MR was less than that measured on CT. In these 52 instances in which the CT scan diameter was greater than the MR diameter, the average difference was 1.04 mm, with an average CT cord diameter of 7.25 mm. The range of differences in these 52 pairs of measurements was 0.17 to 2.3 mm (SD = 1.02 mm) (Fig. 1). The MR diameter exceeded the CT diameter in 18 instances. In 20 levels examined, the AP cord diameter was the same on CT and MR. When all 90 levels were averaged, the mean CT diameter exceeded the mean MR diameter by 0.5 mm (7.25 mm vs 6.75 mm). The difference between the mean CT diameter and the mean MR diameter was statistically significant with a *p* value of .026 on the Student's *t* test.

Normal Volunteers

Of 28 random sections measured in the normal volunteers' cervical spines, the AP diameter of the cord was larger in 23 sections employing a 256 × 256 matrix compared with the 128 × 256 scan with the 128-phase axis oriented in the AP direction (128 AP). The average difference between the measurements was 0.77 mm for all 28 levels measured. In just those levels in which the 256 × 256 scan diameter exceeded that of the 128 AP scan, the average difference was 1.02 mm. The difference between the two measurements ranged from 0.3 to 1.5 mm (SD = 0.50 mm).

TABLE 1: Comparison of AP Diameter of Cord Among Different Imaging Techniques

Study Type	No. of Levels
Patient study	
CT postiohexol AP diameter > 128 AP × 256 right-left MR	52*
CT postiohexol AP diameter = 128 AP × 256 right-left MR	20
CT postiohexol AP diameter < 128 AP × 256 right-left MR	18
MR volunteer study (different matrices)	
1. 256 AP × 256 right-left AP diameter > 128 AP × 256 right-left MR	23*
256 AP × 256 right-left AP diameter = 128 AP × 256 right-left MR	5
256 AP × 256 right-left AP diameter < 128 AP × 256 right-left MR	0
2. 256 AP × 128 right-left AP diameter > 128 AP × 256 right-left MR	21*
256 AP × 128 right-left AP diameter = 128 AP × 256 right-left MR	5
256 AP × 128 right-left AP diameter < 128 AP × 256 right-left MR	2
MR phantom study (different matrices)	
1. 256 AP × 256 right-left AP diameter > 128 AP × 256 right-left MR	13*
256 AP × 256 right-left AP diameter = 128 AP × 256 right-left MR	3
256 AP × 256 right-left AP diameter < 128 AP × 256 right-left MR	0
2. 256 AP × 128 right-left AP diameter > 128 AP × 256 right-left MR	11*
256 AP × 128 right-left AP diameter = 128 AP × 256 right-left MR	3
256 AP × 128 right-left AP diameter < 128 AP × 256 right-left MR	2

Note.—AP = anteroposterior.

* Our comparisons show that the scan with the 128 phase-encoding steps in the AP direction produces a diminution in measured cord diameter. The magnitude of the difference can be as high as 2.3 mm in a 7.5-mm-wide cord.

The AP cord diameter of the 128 × 256 scan with the 128-phase axis oriented right-left (128 right-left) was greater than the AP diameter of the corresponding section in the 128 × 256 scan with the 128-phase axis oriented in the AP direction in 21 of 28 instances. When all 28 sections were examined, the scan cord diameter in the 128 right-left matrix exceeded the 128 AP matrix scan diameter by an average of 0.71 mm. However, the average difference was 0.94 mm in just those 21 instances in which the 128 right-left matrix measurement exceeded the 128 AP matrix. The range of differences in these 21 levels was 0.3 to 1.7 mm (SD = 0.64 mm) (Fig. 2).

Phantom Study

The 256 × 256 matrix AP diameter of the cord phantom was greater in 13 of 16 levels and equal in three levels compared with the 128 × 256 study with the 128-phase axis

in the AP direction. The average overall diameter of the phantom cord was greater by 0.56 mm in the 256 matrix study (average 256 × 256 phantom dimension of 7.3 mm) when all 16 levels were examined. In those 13 levels in which the 256 × 256 measurement exceeded the 128 AP diameter, the average difference was 0.73 mm, with a range of 0.3 to 1.8 mm (SD = 0.48 mm).

When the 128 matrix was right-left, the overall phantom diameter was greater than the 128 AP image in 11 of 16 measurements by an average of 0.50 mm. In just those 11 levels in which the 128 AP scan's diameter was smaller than the 128 right-left study, the average difference was 0.78 mm, with a range of 0.3 to 1.6 mm (SD = 0.56 mm) (Fig. 3). The average CT AP phantom measurement and the direct measurement were within 0.2 mm of the 256 × 256 matrix dimensions, ranging from 7.1 to 7.5 mm.

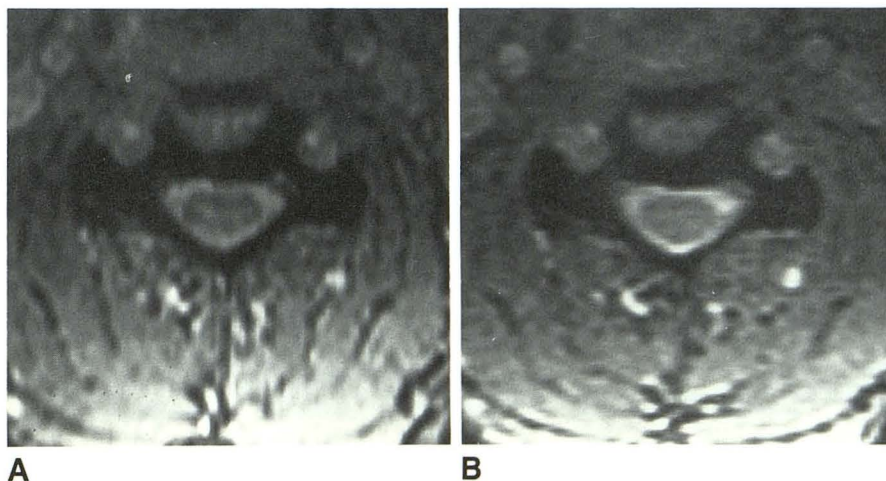
When the window levels and widths were changed on the same 128 AP matrix MR image, it was noted that one could

Fig. 2.—Effect of matrix size on apparent cord dimensions.

A, Gradient-echo volumetric 3DFT scan (50/15/1), 128 (AP) × 256 (right-left).

B, Gradient-echo volumetric 3DFT scan (50/15/1), 256 (AP) × 256 (right-left).

The scan with the 128 axis of a 128 × 256 matrix in the AP direction (A) demonstrates a narrower AP diameter than does the scan at same level with exact same parameters but a 256 × 256 matrix (B). This is due to truncation artifact and photographic windowing to achieve the bright CSF effect. The difference is 1 mm anteroposteriorly between the two scans, but less than 0.1 mm transversely. When the 128 axis is in the right-left direction, the same reduction in diameter is produced in the transverse measurement.



alter the measured cord width by up to 1.5 mm before severe image distortion was produced. This finding was reproducible in the normal volunteer study (Fig. 4).

Discussion

Although the truncation artifact has been well described with respect to its pseudosyrinx appearance on sagittal images of the cervical spinal cord, the impact on spinal cord size on axial images of the spine, and in low flip angle gradient-echo scans, has not been emphasized [1-6].

Truncation artifacts occur at sharp, high-contrast interfaces [1-6]. Whereas the Fourier transformation used in image reconstruction assumes an infinite set of data, in reality, only a finite number of k-space samples are available. The result of this raw data truncation is an oscillatory intensity pattern manifested as a series of alternating bands of low and high signal intensity parallel to the high-contrast interface [1-7]. These intensity bands, appearing in the substance of the cervical spinal cord, create the pseudosyrinx appearance described by previous investigators [2-4, 6]. The characteristic features of this artifact are its regular, periodic spacing and the noticeable drop-off in intensity with successive side

lobes/bands [1, 4, 5, 8]. The Gibbs phenomenon refers to the first undershoot and overshoot intensity waves of the interface, approximately 9% below and above the actual intensity differences of the two structures being examined [1, 3, 4, 8].

The second implication of the truncation artifact and the subject of this paper is the apparent change in the dimensions of objects being imaged when high-contrast interfaces exist. This effect is caused by the sloping of the intensity profile, schematically shown in Figure 5 and evident in the profile calculations in the article by Bronskill et al. [2], which assume rectangular high-contrast objects [3, 9] (Fig. 5). The sloping line of intensity plotted against the distance axis is reinforced when the 128 scanning matrix is interpolated onto a 512 imaging matrix for photography [3, 4, 8, 10]. The sloping line may extend over a minimum of one pixel width (1.875 mm in a 128-matrix scan with a 24-cm FOV) or may extend over more than one pixel in an apodized (filtered) scan [3, 8]. The use of a low-pass, high-frequency filter to attenuate the repetitive side lobes of the signal profile tends to blur high-contrast edges, allowing more potential distortion of cord dimensions by decreasing the slope of the intensity profile through the interface [3, 4, 6, 8]. One may photograph at window settings to create an apparent interface anywhere

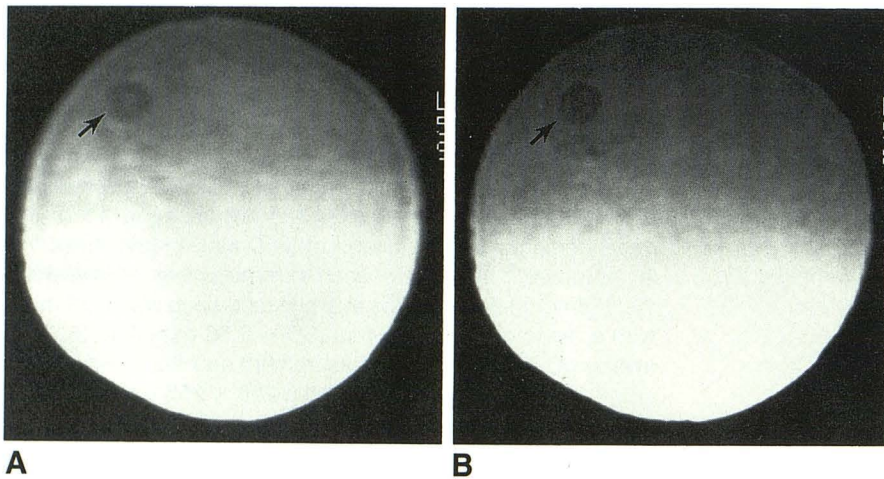


Fig. 3.—Transverse diameter distortion in spine phantom with 128 axis right-left.

A, Gradient-echo volumetric 3DFT scan (50/15/1), 128 (right-left) \times 256 (AP).

B, Gradient-echo volumetric 3DFT scan (50/15/1), 256 (AP) \times 256 (right-left).

The transverse diameter of the agar spinal cord phantom (arrow) in a water bath is truncated in the 128 \times 256 scan when the 128 plane is transverse (A) compared with a 256 \times 256 scan (B) through same level. The phenomenon is not an AP or right-left factor, but dependent on the direction of the 128 axis. A CT scan through the phantom confirmed the accuracy of the 256 \times 256 dimensions.

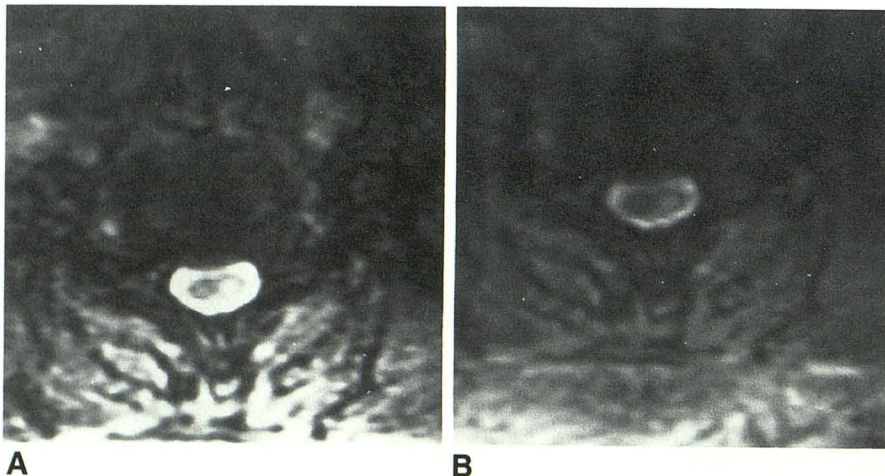


Fig. 4.—Effect of photographic windowing on apparent cord size.

A, Gradient-echo volumetric 3DFT scan (50/15/1), 128 (AP) \times 256 (right-left), narrow window settings.

B, Gradient-echo volumetric 3DFT scan (50/15/1), 128 (AP) \times 256 (right-left), with wide window settings.

These two images (A and B) are at exact same level with exact same scanning parameters, but are photographed with a narrow window and level (A) or a wide window and level (B). Note apparent increase in cord diameter in the darker image (B) and pseudoatrophic appearance in the scan with the more hyperintense CSF (A). Anatomic detail is lost with wider windowing.

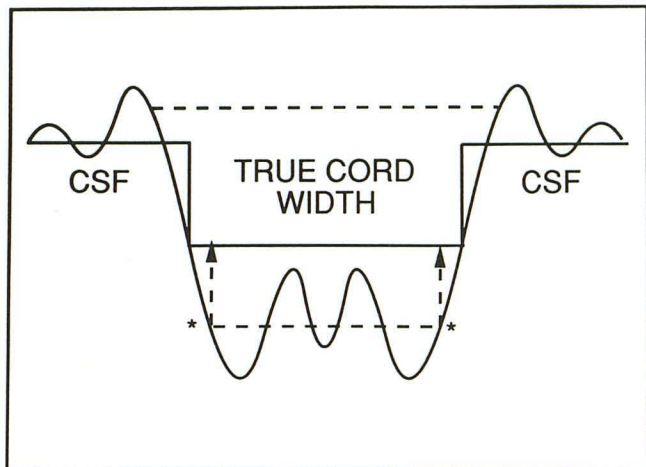


Fig. 5.—Diagrammatic representation of mechanism of pseudoatrophy. The sloping line of the Fourier transformation intensity profile between CSF and spinal cord will extend across at least one pixel width. In a scan with a 24-cm FOV and a 128×256 matrix, one pixel width is 1.875 mm, producing a flatter slope than if a 256×256 matrix (0.9375 mm pixel) were used. The cord may be photographed within the range of intensity levels shown as dotted lines, which inaccurately display the true cord width. To produce the bright CSF intensity desired for a myelographic effect, one usually photographs at the lower window level (asterisks), thereby producing an underestimation of cord diameter.

along this sloping line, leading to misrepresentation of true cord width. The potential for misrepresentation of cord size is lessened with the use of a 256×256 matrix scan owing to the sampling of higher spatial frequencies; however, it does persist and its magnitude is dependent on operator-determined photographic window settings.

The methods for reducing truncation artifacts include decreasing the pixel diameter by increasing the matrix size or decreasing the field of view [1–6, 8, 9]. Alternatively, one may change frequency and phase-encoding axes to divert the artifact to a less confusing plane with the smaller sampling frequency [2, 4, 6, 7]. Although this artifact is exaggerated on long TR/TE and short flip angle gradient-echo images of the spinal cord, it is expected to occur on short TR/TE images as well. The presence of a pseudosyrinx on sagittal short TR/TE spin-echo scans attests to the truncation artifact's persistence on these sequences. Even if the 128 phase-encoding steps were able to be represented perfectly as a perpendicular

step function at the cord-CSF interface, the interpolation of points between the two high-contrast intensity points during conversion of the data onto a standard 512×512 display format will create the potential for misrepresentation of absolute cord measurements through photographic windowing on the monitors.

In summary, the truncation artifact creates the potential for misrepresenting the cord-CSF interface because of the sloping of the intensity profile. This sloping line of intensity is perpetuated by interpolation of 128 matrix points onto a 512 photographic matrix. By attempting to achieve high-contrast images of the spine, window settings may be selected at which the apparent spinal cord size is reduced.

It is critically important to recognize the truncation effect in the axial examination of the cervical spine. Because the cord's dimensions may be inaccurately depicted on these MR images, the potential exists for overdiagnosing spinal cord atrophy or compression. The neuroradiologist must therefore be wary of conclusions based on spinal cord measurements or cord morphology obtained while using a relatively small matrix scan.

REFERENCES

1. Wood ML, Henkelman RM. Truncation artifacts in magnetic resonance imaging. *Magn Reson Med* 1985;2:517–526
2. Bronskill MJ, McVeigh ER, Kucharczyk W, Henkelman RM. Syrinx-like artifacts on MR images of the spinal cord. *Radiology* 1988;166:485–488
3. Levy LM, Di Chiro G, Brooks RA, Dwyer AJ, Wener L, Frank J. Spinal cord artifacts from truncation errors during MR imaging. *Radiology* 1988;166:479–483
4. Czervionke LF, Czervionke JM, Daniels DL, Houghton VM. Characteristic features of MR truncation artifacts. *AJNR* 1988;9:815–824
5. Curtin AJ, Chakeres DW, Bulas R, Boesel CP, Finneran M, Flint E. MR imaging artifacts of the axial internal anatomy of the cervical spinal cord. *AJNR* 1989;10:19–26
6. Henkelman RM, Bronskill MJ. Artifacts in magnetic resonance imaging. *Rev Magn Reson Med* 1987;2:1–126
7. Haacke EM. The effects of finite sampling in spin-echo or field-echo magnetic resonance imaging. *Magn Reson Med* 1987;4:407–421
8. Lufkin RB, Pusey E, Stark DD, Brown R, Leikind B, Hanafee WN. Boundary artifact due to truncation errors in MR imaging. *AJR* 1986;147:1283–1287
9. Breger RK, Czervionke LF, Kass EG, et al. Truncation artifact in MR images of the intervertebral disk. *AJNR* 1988;9:825–828
10. Gellad F, Rao KCVG, Joseph PM, Vigorito RD. Morphology and dimensions of the thoracic cord by computer-assisted metrizamide myelography. *AJNR* 1983;4:614–617